

Efficient $O(N^{1.5})$ Electronic Structure Computation of Million-Atom Systems

Zichong Zhang¹, Shuze Zhu*¹

¹Center for X-Mechanics, Department of Engineering Mechanics,

Zhejiang University, Hangzhou 310000, China

*To whom correspondence should be addressed. E-mail: shuzezhu@zju.edu.cn

Abstract

The exploration of quantum phenomena in complex materials such as moiré superlattices is limited by the $O(N^3)$ scaling of conventional electronic structure methods. Here we introduce a high-performance tight-binding framework that reduces the complexity to $O(N^{1.5})$ by transforming the Hamiltonian into a real symmetric form and combining Sylvester's inertia law with LDL decomposition. This approach enables efficient band structure calculations for large systems—solving magic-angle twisted bilayer graphene in minutes on a laptop and scaling to 1.5 million atoms within days on a workstation. We apply it to the previously inaccessible ultra-low twist-angle regime ($<0.16^\circ$) with mechanical strain relaxation and find robust flat bands persisting down to 0.09° . Our framework bridges density functional theory accuracy with large-scale quantum simulation, opening a route to systematic data-driven exploration of mesoscale quantum materials.

Introduction — The electronic properties of modern quantum materials are increasingly governed by physics at the mesoscopic scale. Prominent examples range from flat bands and correlated states in twisted van der Waals heterostructures to topologically protected phases in disordered systems [1–7]. Understanding these phenomena requires an accurate description of electronic structures in systems where the unit cell can contain hundreds of thousands to millions of atoms—a scale at which computational cost becomes a formidable barrier.

While density functional theory (DFT) provides a first-principles foundation, its high computational load restricts it to systems of $10^2 - 10^3$ atoms [8,9]. Tight-binding (TB) models strike a balance between accuracy and efficiency and have been widely used for larger systems [10]. Nevertheless, conventional TB methods still rely on explicit diagonalization of the Hamiltonian matrix, which scales as $O(N^3)$. This limits even TB simulations typically to $10^4 - 10^5$ atoms, leaving a significant “scale gap” to real nanostructures. For example, in twisted bilayer graphene (TBG) at angles below 0.3° , the moiré period extends to tens of nanometers, requiring the treatment of hundreds of thousands of atoms to capture electronic coupling and structural relaxation.

In this Letter, we introduce a computational framework that breaks the $O(N^3)$ bottleneck and enables tight-binding band-structure calculations at the million-atom scale. The key idea lies in converting the sparse Hermitian Hamiltonian into a real symmetric form, which then allows the use of efficient LDL decomposition together with Sylvester’s inertia law to locate the Fermi energy without full diagonalization. By further integrating the shift-invert Arnoldi

method to extract bands near the Fermi level, we achieve an overall scaling of approximately $O(N^{1.5})$. This efficiency makes large-scale quantum simulation practical: calculating the band structure for a magic-angle TBG system ($\sim 11,000$ atoms) takes about one minute on a laptop, while solving a 1.5-million-atom system over approximately 100 k -points requires about two days on a workstation.

We demonstrate the capability of our method by applying it to a series of TBG structures at ultra-low twist angle ranges—a regime previously inaccessible to ab initio or conventional TB approaches. We show that with atomistic structural relaxation the flat bands persist robustly down to angle 0.09° . Our work bridges the gap between local DFT accuracy and macroscopic quantum scales, providing a scalable computational framework that supports both fundamental studies and data-driven discovery of mesoscopic phenomena in complex materials [11–13].

Computational methods —The computational workflow comprises four general stages applicable to any periodic system described by a real-space tight-binding Hamiltonian. Starting from an atomic structure under periodic boundary conditions, the first step is to construct the sparse Hermitian Hamiltonian matrix using KD-tree-accelerated neighbor search [14], crucial for treating large systems. The second step involves converting the Hermitian Hamiltonian into a real symmetric form. This critical transformation enables the direct application of LDL decomposition together with Sylvester’s law of inertia to locate the Fermi level without full diagonalization. The third step employs the shift-invert Arnoldi method [15,16] to extract eigenvalues near the Fermi level. Finally, the band structure across

the Brillouin zone can be computed in parallel for further acceleration. With $O(N^{1.5})$ scaling for 2D systems, our approach enables high-throughput band structure calculations over ~ 100 k -points within practical timeframes: from about one minute for a magic-angle TBG system ($\sim 1.1 \times 10^4$ atoms) on a laptop, to roughly two days for a 1.5-million-atom system on a workstation.

For a periodic supercell of N atoms, the tight-binding Hamiltonian H is sparse since the hopping integral t_{ij} is significant only within a finite cutoff distance r_c . A direct calculation of all pairwise distances would scale as $O(N^2)$. We reduce this to $O(N \log N)$ by employing a KD-Tree spatial indexing algorithm [14] to partition the cell. For each atom i , we identify all neighbors j (including those in adjacent periodic images) that satisfy $|\mathbf{r}_i - \mathbf{r}_j| < r_c$. The corresponding hopping matrix elements are computed and stored in Compressed Sparse Column format. This sparse template is constructed once and reused for all wavevectors \mathbf{k} .

For large systems, we are primarily interested in electronic states near the Fermi energy E_F . Instead of performing a full $O(N^3)$ diagonalization, we determine E_F by finding the energy ε below which exactly N_{occ} eigenvalues of the original Hamiltonian lie (typically $N_{occ} = N/2$ for a neutral system). Formally, for a Hamiltonian at a suitable reference wavevector \mathbf{k}_0 , this is equivalent to computing the inertia of $H(\mathbf{k}_0) - \varepsilon I$.

However, because H is complex Hermitian, the LDL decomposition required by Sylvester's inertia law [17] cannot be applied directly. This limitation motivates the critical transformation in our approach: we convert the $N \times N$ complex Hermitian matrix into a

$2N \times 2N$ real symmetric matrix of the form

$$H_{real} = \begin{pmatrix} Re(H) & -Im(H) \\ Im(H) & Re(H) \end{pmatrix}, \quad (1)$$

which maps each eigenvalue of H to a two-fold degenerate eigenvalue of H_{real} (see details in Appendix). Consequently, the inertia—and thus the integrated density of states (IDOS)—of the shifted matrices satisfies $\text{Inertia}(H_{real} - \varepsilon I) = 2 \cdot \text{Inertia}(H - \varepsilon I)$, preserving the full spectral information of the original quantum system while enabling the use of high-performance real-symmetric LDL solvers.

H_{real} plays a critical role within our framework. Beginning with an initial guess ε_0 , we compute the LDL decomposition of $H_{real} - \varepsilon_0 I$ using a fill-reducing ordering. The resulting matrix D is block diagonal. By scanning the diagonal blocks of D , we rapidly obtain the total counts N_{neg} of negative eigenvalues of D . The value of ε_0 is then updated iteratively until $N_{neg} = N_{occ}$, thereby determining the Fermi energy E_F . For a two-dimensional sparse periodic Hamiltonian, the LDL step scales as $O(N^{1.5})$, constituting the central complexity reduction of our algorithm.

Once E_F is determined, the band structure near this energy can be computed. For each wavevector \mathbf{k} along a chosen symmetry path, we assemble $H(\mathbf{k})$ by combining the precomputed hopping integrals with phase factors $e^{i\mathbf{k}\cdot\mathbf{d}}$, where \mathbf{d} is the interatomic hopping vector including periodic images. The shift-invert Arnoldi method [15,16] is then applied to solve $(H(\mathbf{k}) - \sigma I)^{-1}x = vx$ with shift $\sigma = E_F$. Each Arnoldi iteration requires the solution of a linear system $(H(\mathbf{k}) - \sigma I)y = x$. Sparse matrices of up to a million atoms can be solved

efficiently using a high-performance sparse direct solver. Owing to the favorable sparsity pattern inherent to two-dimensional lattices, the computational cost per k -point retains an $O(N^{1.5})$ scaling—a substantial improvement over the conventional $O(N^3)$ bottleneck [18] associated with dense eigen solvers.

Twisted bilayer graphene with extremely small angles — Our method is applied to explore the previously inaccessible regime of twisted bilayer graphene (TBG). The TBG structure is commonly described by a pair of integers (m, n) that defines its moiré unit cell [19]. In this Letter, we focus on configurations satisfying $n = m + 1$. The tight-binding Hamiltonian is written as

$$H = \sum_{i,j} t(\mathbf{R}_i - \mathbf{R}_j) |\mathbf{R}_i\rangle\langle\mathbf{R}_j| + H. c., \quad (2)$$

where \mathbf{R}_i denotes atomic coordinate and $|\mathbf{R}_i\rangle$ is the wavefunction at site i . $t(\mathbf{R}_i - \mathbf{R}_j)$ is the transfer integral between atoms i and j . From standard Slater-Koster formula there is [20],

$$\begin{aligned} t(\mathbf{d}) &= V_{pp\pi}(d) \left[1 - \left(\frac{\mathbf{d} \cdot \mathbf{e}_z}{d} \right)^2 \right] + V_{pp\sigma}(d) \left(\frac{\mathbf{d} \cdot \mathbf{e}_z}{d} \right)^2, \\ V_{pp\pi}(d) &= V_{pp\pi}^0 e^{\left(-\frac{d-a}{\delta} \right)}, \\ V_{pp\sigma}(d) &= V_{pp\sigma}^0 e^{\left(-\frac{d-d_0}{\delta} \right)}. \end{aligned} \quad (3)$$

where $\mathbf{d} = \mathbf{R}_i - \mathbf{R}_j$ is interatomic hopping vector (including periodic images), and \mathbf{e}_z is unit vector parallel to z -axis.

We adopt parameters from Moon and Koshino [19], with $V_{pp\pi}^0 = -2.7 \text{ eV}$, $V_{pp\sigma}^0 = 0.48 \text{ eV}$, $d_0 = 0.335 \text{ nm}$, $\delta = 0.184\sqrt{3}a_0$ ($a_0 = 0.142 \text{ nm}$ is carbon-carbon bond length).

The transfer integral is neglected for $d > 4a_0$.

To incorporate mechanical strain relaxation, we optimize the atomic structures using LAMMPS [21]. Intra-layer interactions are described by the REBO potential [22], while the inter-layer interactions are modeled with the registry-dependent interlayer potential (ILP) [23]. Energy minimization is performed via the conjugate gradient algorithm, continuing until the relative change in total energy between successive iterations falls below 10^{-13} .

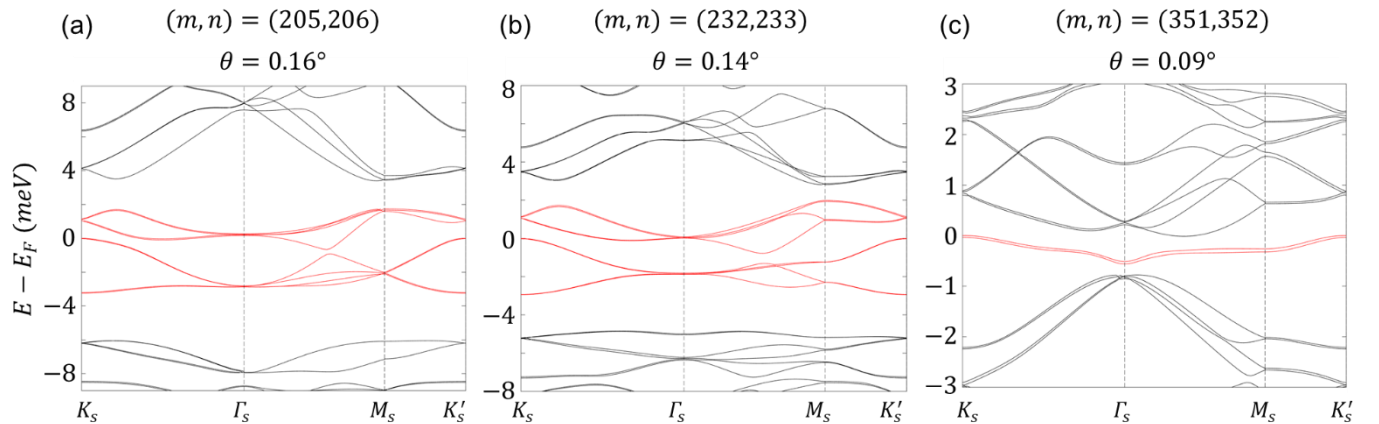


Figure 1. The electronic band structures of large-scale relaxed twisted bilayer graphene with extremely small angles. (a) $(m, n) = (205, 206)$ with twist angle 0.16° . (b) $(m, n) = (232, 233)$ with twist angle 0.14° . (c) $(m, n) = (350, 351)$ with twist angle 0.09° . The red lines indicate the flat bands near the Fermi level.

Figure 1 presents the calculated band structures for relaxed TBG with extremely small twist angles below 0.16° . The largest system contains more than 1.5 million atoms (corresponding to 0.09°), with a length scale of 150 nm. In this regime, a set of flat bands emerges near the

Fermi level. Further calculations reveal that these flat bands emerge within discrete angular windows—for instance, between 0.14° and 0.16° , and near 0.09° . These results reveal flat-band regions at angles that are, to our knowledge, previously unreported [7], a gap attributable to the challenge of treating large-scale, atomistically relaxed systems.

Scaling performance — To assess the scaling performance of our algorithm, we construct a series of moiré unit cells in twisted bilayer graphene by systematically varying the twist vector specified by integer pairs (m, n) . Figure 2 shows the computed time required to obtain 40 bands near the Fermi level for the two main algorithmic steps: LDL decomposition of the transformed real symmetric Hamiltonian [Fig. 2(a)] and shift-invert eigenvalue extraction near the Fermi level [Fig. 2(b)]. Both operations are found to scale as $O(N^{1.5})$. Consequently, the total computation time [Fig. 2(c)] also follows an approximately $O(N^{1.5})$ scaling with the number of atoms.

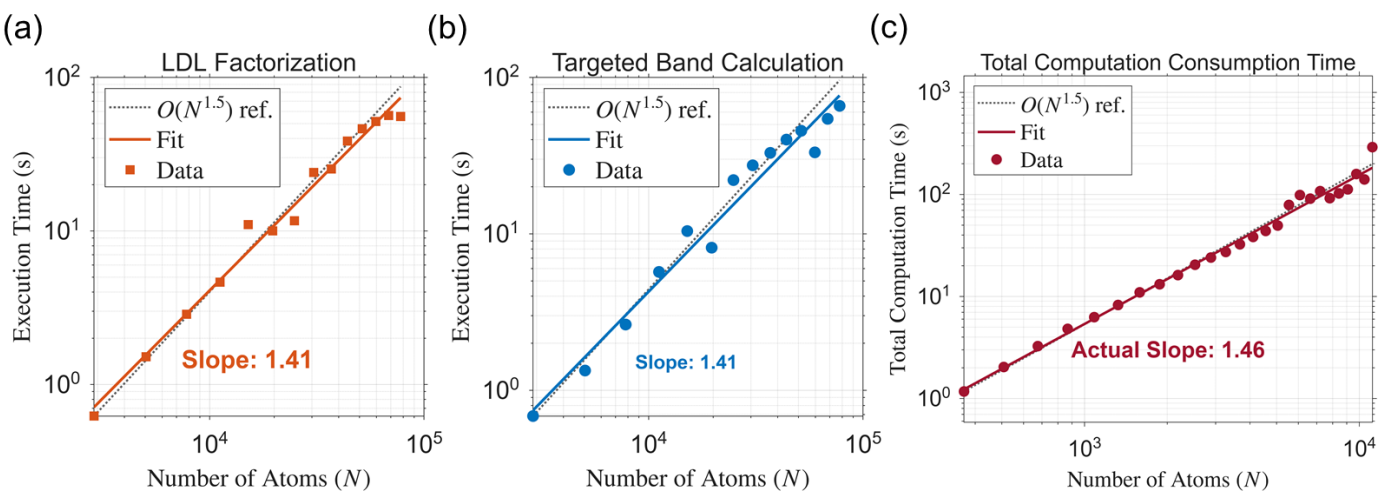


Figure 2. Scaling performance of the twisted bilayer graphene system. (a) LDL decomposition of converted real symmetric Hamiltonian. (b) Shift-Invert for eigenvalue extraction near the Fermi level. (c) Total computation time.

Conclusion —This Letter presents a scalable computational framework for large-scale electronic structure calculations. The complexity is reduced to $O(N^{1.5})$ by transforming the Hamiltonian into a real symmetric form and employing an inertia-based spectral slicing scheme via LDL decomposition and Sylvester’s law. This advance enables electronic structure calculations for systems beyond one million atoms, effectively bridging the scale gap between first-principles accuracy and mesoscopic sample dimensions.

Our method establishes a versatile computational platform for quantum materials research. High-fidelity local electronic parameters obtained from small-scale density functional theory (DFT) calculations can be directly incorporated into this scalable framework, allowing systematic exploration of macroscopic quantum phenomena—such as the evolution of flat bands and soliton networks in ultra-low-angle twisted bilayer graphene—that were previously beyond the reach of both *ab initio* and conventional tight-binding approaches. Furthermore, the algorithm provides a reliable source of large-scale, first-principles-informed data for training and validating next-generation data-driven models, including neural networks for band-gap and electronic-state prediction. By extending quantum-accurate simulations to experimentally relevant length scales, this work opens a practical route toward data-driven discovery in complex materials.

Appendix: Derivation of the Inertia Relation

Let H be an $N \times N$ complex Hermitian matrix, which can be decomposed into real and imaginary parts:

$$H = A + iB,$$

where A is a real symmetric matrix ($A^\top = A$) and B is a real skew-symmetric matrix ($B^\top = -B$). We construct a $2N \times 2N$ real symmetric block matrix:

$$H_{real} = \begin{pmatrix} A & -B \\ B & A \end{pmatrix}.$$

Suppose λ is an eigenvalue of H with the corresponding eigenvector $\mathbf{x} = \mathbf{u} + i\mathbf{v} \in \mathbb{C}^N$ ($\mathbf{u}, \mathbf{v} \in \mathbb{R}^N$). Then

$$H\mathbf{x} = \lambda\mathbf{x}.$$

Separating the real and imaginary parts gives:

$$A\mathbf{u} - B\mathbf{v} = \lambda\mathbf{u},$$

$$B\mathbf{u} + A\mathbf{v} = \lambda\mathbf{v}.$$

These two equations can be written in block form as

$$\begin{pmatrix} A & -B \\ B & A \end{pmatrix} \begin{pmatrix} \mathbf{u} \\ \mathbf{v} \end{pmatrix} = \lambda \begin{pmatrix} \mathbf{u} \\ \mathbf{v} \end{pmatrix},$$

which shows that λ is an eigenvalue of H_{real} with a real eigenvector $(\mathbf{u}, \mathbf{v})^\top$.

Moreover, multiplying the eigenvector \mathbf{x} by i yields $i\mathbf{x} = -\mathbf{v} + i\mathbf{u}$, corresponding to the real vector $(-\mathbf{v}, \mathbf{u})^\top$, which also satisfies

$$\begin{pmatrix} A & -B \\ B & A \end{pmatrix} \begin{pmatrix} -\mathbf{v} \\ \mathbf{u} \end{pmatrix} = \lambda \begin{pmatrix} -\mathbf{v} \\ \mathbf{u} \end{pmatrix}.$$

Since $(\mathbf{u}, \mathbf{v})^\top$ and $(-\mathbf{v}, \mathbf{u})^\top$ are linearly independent, the eigenvalue λ has double algebraic multiplicity in H_{real} . The whole spectrum of H_{real} consists of each eigenvalue of H repeated twice.

For any real shift parameter ε , consider the shifted matrices $H - \varepsilon I_N$ and $H_{real} - \varepsilon I_{2N}$. The eigenvalues of $H - \varepsilon I_N$ are $\{\lambda_i - \varepsilon\}$, while those of $H_{real} - \varepsilon I_{2N}$ are $\{\lambda_i - \varepsilon, \lambda_i - \varepsilon\}$ (each eigenvalue of H appears twice).

The inertia of a matrix—defined as the triple (v_+, v_-, v_0) counting its positive, negative, and zero eigenvalues, respectively—therefore satisfies

$$Inertia(H_{real} - \varepsilon I_{2N}) = 2 \cdot Inertia(H - \varepsilon I_N).$$

Consequently, the integrated density of states (IDOS) obtained from the inertia of the shifted real symmetric matrix is exactly twice that obtained from the original Hermitian matrix, preserving the full spectral information needed to locate the Fermi energy.

This relation justifies the use of the real symmetric form H_{real} in conjunction with Sylvester's inertia law. The factor of 2 is accounted for by adjusting the target electron count when determining the Fermi level.

Reference

- [1] Y. Cao, V. Fatemi, S. Fang, K. Watanabe, T. Taniguchi, E. Kaxiras, and P. Jarillo-Herrero, Unconventional superconductivity in magic-angle graphene superlattices, *Nature* **556**, 43 (2018).
- [2] Y. Choi et al., Electronic correlations in twisted bilayer graphene near the magic angle, *Nat. Phys.* **15**, 1174 (2019).
- [3] J. M. Park, Y. Cao, K. Watanabe, T. Taniguchi, and P. Jarillo-Herrero, Tunable strongly coupled superconductivity in magic-angle twisted trilayer graphene, *Nature* **590**, 249 (2021).
- [4] A. Uri et al., Mapping the twist-angle disorder and Landau levels in magic-angle graphene, *Nature* **581**, 47 (2020).
- [5] Y. Xie, B. Lian, B. Jäck, X. Liu, C.-L. Chiu, K. Watanabe, T. Taniguchi, B. A. Bernevig, and A. Yazdani, Spectroscopic signatures of many-body correlations in magic-angle twisted bilayer graphene, *Nature* **572**, 101 (2019).
- [6] J. Mao et al., Evidence of flat bands and correlated states in buckled graphene superlattices, *Nature* **584**, 215 (2020).
- [7] R. Bistritzer and A. H. MacDonald, Moiré bands in twisted double-layer graphene, *Proc. Natl. Acad. Sci. U.S.A.* **108**, 12233 (2011).
- [8] J. Pan, Scaling up system size in materials simulation, *Nat Comput Sci* **1**, 95 (2021).
- [9] T. Müller, S. Sharma, E. K. U. Gross, and J. K. Dewhurst, Extending Solid-State Calculations to Ultra-Long-Range Length Scales, *Phys. Rev. Lett.* **125**, 256402 (2020).
- [10] S. Carr, S. Fang, and E. Kaxiras, Electronic-structure methods for twisted moiré layers, *Nat Rev Mater* **5**, 748 (2020).
- [11] E. Tsymbalov, Z. Shi, M. Dao, S. Suresh, J. Li, and A. Shapeev, Machine learning for deep elastic strain engineering of semiconductor electronic band structure and effective mass, *Npj Comput Mater* **7**, 76 (2021).
- [12] L. Zhang, T. Su, M. Li, F. Jia, S. Hu, P. Zhang, and W. Ren, Accurate band gap prediction based on an interpretable Δ -machine learning, *Materials Today Communications* **33**, 104630 (2022).
- [13] Y. Dong, C. Wu, C. Zhang, Y. Liu, J. Cheng, and J. Lin, Bandgap prediction by deep learning in configurationally hybridized graphene and boron nitride, *Npj Comput Mater* **5**, 26 (2019).
- [14] S. Arya, D. M. Mount, N. S. Netanyahu, R. Silverman, and A. Y. Wu, An optimal algorithm for approximate nearest neighbor searching fixed dimensions, *J. ACM* **45**, 891 (1998).
- [15] T. Ericsson and A. Ruhe, The Spectral Transformation Lanczos Method for the Numerical Solution of Large Sparse Generalized Symmetric Eigenvalue Problems, *Mathematics of Computation* **35**, 1251 (1980).
- [16] R. B. Lehoucq, D. C. Sorensen, and C. Yang, *ARPACK Users' Guide* (Society for Industrial and Applied Mathematics, 1998).

- [17] A. M. Ostrowski, A quantitative formulation of sylvester's law of inertia*, Proceedings of the National Academy of Sciences **45**, 740 (1959).
- [18] S. Goedecker, Linear scaling electronic structure methods, Rev. Mod. Phys. **71**, 1085 (1999).
- [19] P. Moon and M. Koshino, Energy spectrum and quantum Hall effect in twisted bilayer graphene, Phys. Rev. B **85**, 195458 (2012).
- [20] J. C. Slater and G. F. Koster, Simplified LCAO Method for the Periodic Potential Problem, Phys. Rev. **94**, 1498 (1954).
- [21] A. P. Thompson et al., LAMMPS - a flexible simulation tool for particle-based materials modeling at the atomic, meso, and continuum scales, Computer Physics Communications **271**, 108171 (2022).
- [22] D. W. Brenner, O. A. Shenderova, J. A. Harrison, S. J. Stuart, B. Ni, and S. B. Sinnott, A second-generation reactive empirical bond order (REBO) potential energy expression for hydrocarbons, J. Phys.: Condens. Matter **14**, 783 (2002).
- [23] W. Ouyang, D. Mandelli, M. Urbakh, and O. Hod, Nanoserpents: Graphene Nanoribbon Motion on Two-Dimensional Hexagonal Materials, Nano Lett. **18**, 6009 (2018).